Determining Near-Surface Soil Heat Flux Density Using the Gradient Method: A Thermal Conductivity Model–Based Approach

XIAOYANG PENG

Department of Soil and Water Sciences, China Agricultural University, Beijing, China

JOSHUA HEITMAN

Crop and Soil Sciences Department, North Carolina State University, Raleigh, North Carolina

ROBERT HORTON

Department of Agronomy, Iowa State University, Ames, Iowa

TUSHENG REN

Department of Soil and Water Sciences, China Agricultural University, Beijing, China

(Manuscript received 15 December 2016, in final form 17 May 2017)

ABSTRACT

In the gradient method, soil heat flux density at a known depth G is determined as the product of soil thermal conductivity λ and temperature T gradient. While measuring λ in situ is difficult, many field studies readily support continuous, long-term monitoring of soil T and water content θ in the vadose zone. In this study, the performance of the gradient method is evaluated for estimating near-surface G using modeled λ and measured T. Hourly λ was estimated using a model that related λ to θ, soil bulk density ρ_b, and texture at 2-, 6-, and 10-cm depths. Soil heat flux G_m was estimated from modeled λ and measured T gradient (from thermocouples). The G_m results were evaluated with heat flux data G_{HP} determined using independent measured λ and T gradient from heat-pulse probes. The λ model performed well at the three depths with 3.3%–7.4% errors. The G_m estimates were similar to G_{HP} (agreed to within 15.1%), with the poorest agreement at the 2-cm soil depth, which was caused mainly by the relatively greater variability in ρ_b. Accounting for temporal variations in ρ_b (with core method) improved the accuracies of λ and G_m at the 2-cm depth. Automated θ monitoring approaches (e.g., time domain reflectometry), rather than gravimetric sampling, captured the temporal dynamics of near-surface λ and G well. It is concluded that with continuous θ and T measurements, the λ model–based gradient method can provide reliable near-surface G. Under conditions of soil disturbance or deformation, including temporally variable ρ_b, data improves the accuracy of G data.

1. Introduction

The surface energy balance (SEB) drives the dynamics of water, energy, and biogeochemical cycles near the Earth's surface. As a key component of the SEB, soil heat flux at the land surface G_0 is important in modulating hydrological, ecological, and atmospheric processes (Gentine et al. 2012; Wang and Bou-Zeid 2012). Commonly, G_0 is determined using the combination method, which includes soil heat flux density at a depth G a few centimeters below the surface, the rate of heat storage change in the soil layer above the G measurement depth, and correction of latent heat flux consumed by evaporation (if the evaporation front is below G measurement depth; Mayocchi and Bristow 1995; Ochsner et al. 2007; Heitman et al. 2010). Reliable G estimates are required for determining G_0 accurately with the combination method (Sauer and Horton 2005; Ochsner et al. 2006).

The gradient method, which is based on Fourier's law, has been applied to determine G from measurements of soil thermal conductivity λ and temperature gradient ($\Delta T/\Delta z$; where T indicates temperature and z indicates depth). Soil temperature can be measured using

Corresponding author: Tusheng Ren, tsren@cau.edu.cn

DOI: 10.1175/JHM-D-16-0290.1

temperature sensors with a relatively high accuracy (McInnes 2002). Determining λ can be difficult, as it changes temporally and spatially by a factor of 2–5 under the influences of soil texture, mineral composition, volumetric water content θ, bulk density ρ_b, and salt content (Abu-Hamdeh and Reeder 2000; Sauer 2002). A few studies have investigated the effects of λ determination on G with the gradient method (Kimball et al. 1976; Peters-Lidard et al. 1998; Evett et al. 2012) and suggest that the reliability of G depends largely on the accuracy of λ. However, the difficulties in obtaining reliable and dynamic λ usually limit the application and accuracy of the gradient method in the field.

The heat-pulse probe (HPP) has been shown to work well in obtaining λ and G for rigid soils under field conditions (Cobos and Baker 2003; Ochsner et al. 2006; Heitman et al. 2008; Peng et al. 2015). This approach has the advantages of providing in situ and continuous λ with minimum soil disturbance and permitting collocated and concurrent measurements of λ and $\Delta T/\Delta z$. Also, several corrections are available for minimizing measurement errors associated with the HPP technique (e.g., ambient temperature drift, soil-probe thermal contact resistance, finite probe properties, and soil–air interface; Jury and Bellantuoni 1976; Bristow et al. 1993; Liu et al. 2013; Lu et al. 2013; Zhang et al. 2014). The HPP method, however, requires substantial instrumentation and data processing.

Soil thermal conductivity models (e.g., Johansen 1975; Chung and Horton 1987; Côté and Konrad 2005) provide an alternative way for estimating λ from easily measurable soil parameters such as texture, θ, and ρ_b. For example, an improved Johansen (1975) model presented by Lu et al. (2007) provided reliable λ using texture, θ, and ρ_b. This model has been applied in studies of coupled heat and water transfer in soils (Farhadi et al. 2014; Dong et al. 2015). A simple model developed by Lu et al. (2014, hereafter L14) estimates λ for soils with various soil textures and different ρ_b values across a wide θ range. Laboratory tests showed that these simple models provide reliable λ estimates with comparable accuracy to those obtained using the HPP. Therefore, λ models have potential for determining G. However, there is a lack of information about performance and potential error sources for application of the λ model–based gradient method under field conditions.

In this study, we introduce a λ model–based gradient method for determination of G in the near-surface soil layer. The new approach is evaluated using the HPP-based gradient method as a reference. The effects of ρ_b and θ data inputs on λ and G results are also assessed.

2. Materials and methods

a. Soil thermal conductivity model

In this study, the L14 model was used to estimate the dynamics of λ. We chose this model for its relatively high accuracy, ease of use, and the capability of describing λ as a function of variable ρ_b and θ.

L14 developed an empirical model for estimating λ with an exponential function:

$$\lambda = \lambda_{\text{dry}} + \exp(\beta - \theta^{-\alpha}), \tag{1}$$

where λ_{dry} is the thermal conductivity of dry soils ($\text{W m}^{-1}\text{K}^{-1}$) and α (related to clay fraction of soil f_c) and β (related to quartz fraction of soil f_q and ρ_b) are shape factors of the λ (θ) curve.

A linear function is used to determine λ_{dry} from soil porosity n:

$$\lambda_{\text{dry}} = -0.56n + 0.51. \tag{2}$$

The shape factors can be determined using the following functions:

$$\alpha = 0.67f_c + 0.24 \quad \text{and} \tag{3}$$

$$\beta = 1.97f_q + 1.87\rho_b - 1.36f_q\rho_b - 0.95. \tag{4}$$

We assumed that the soil sand fraction f_s could serve as a proxy for f_q, and thus, f_s was used in place of f_q in Eq. (4).

b. Field site and soil physical attributes

The field study was performed at the experimental farm of China Agricultural University (40°N, 116°E). The soil has a sandy loam texture with 79.8%, 7.9%, and 12.3% sand, silt, and clay, respectively. Before sensor installation on day of year (DOY) 233 in 2014, the soil was tilled to a 10-cm depth. Three parameters, soil texture (f_s and f_c), ρ_b, and θ are required for the L14 model. The values of f_s and f_c were determined with the pipette method (Gee and Or 2002). Information about sampling depth and frequency for soil bulk density and water content is listed in Table 1. The value of ρ_b was determined by sampling the soil from DOY 253 to 278, with an average interval of 1.9 days. Soil cores from the 0–5- and 5–10-cm soil layers were collected with core samplers (5 cm diameter and 5 cm high, three replicates for each layer), oven dried at 105°C for 24 h, and weighed to determine ρ_b. A meteorological station at the site provided precipitation data with a tipping-bucket rain gauge.

c. Soil water content measurement

Hourly θ measurements at 2-, 6-, and 10-cm depths were collected using a time domain reflectometer (TDR;

TABLE 1. Soil bulk density and water content measurement intervals, depths, and methods in the L14 model.

Model input parameter	Interval	Depth (cm)	Method
ρ_b (g cm^{-3})	1.9 days	0–5 and 5–10	Core method (Grossman and Reinsch 2002)
θ (cm^3 cm^{-3})	1.0 h	2, 6, and 10	TDR (Ferré and Topp 2002)
	1.9 days	2, 6, and 10	Gravimetric sampling (Zhang et al. 2014)

TDR100, Campbell Scientific, Logan, Utah) and three TDR probes at each depth. The TDR probe has three rods, with a rod diameter of 0.2 cm, a length of 7.5 cm, and rod-to-rod spacing of 2 cm. At each measurement, the time domain reflectometer applied a fast rise time electromagnetic pulse to the TDR probe, then received reflected pulse signals and estimated dielectric constant of the soil based on the ratio of apparent rod length (product of velocity and travel time of pulse signals) to real rod length. The dielectric constant estimates were recorded by a datalogger (CR23X, Campbell Scientific, Logan, Utah) automatically and were used to estimate soil volumetric water contents with the equation presented by Topp et al. (1980). At each depth, volumetric water content measurements were the mean values of data from three TDR probes.

We also used a soil core sample device (Zhang et al. 2014) to collect soil samples for measuring centimeter-scale gravimetric water content. The device consists of a cylindrical soil core sampler (5 cm diameter and 10 cm high) with a thin hard plastic liner (open cylinder shape) taped tightly onto the inner wall (Fig. 1). Before attaching the plastic liner, straight lines were drawn in the vertical direction (the dashed lines), which served as marks for cutting the soil sample into layers. To collect the samples, the upper 1-cm soil layer was removed, and then the sampler was pushed into the 1–11-cm soil layer. The core sampler has a sharp, inward-beveled cutting edge at the bottom end, which helps to minimize the resistance and soil compaction during insertion. After excavating the sampler, the soil core within the plastic liner was taken out carefully, cut into 1–3-, 5–7-, and 9–11-cm depth increments, weighed, and oven dried at 105°C for 24 h to determine gravimetric water contents at depths of 2, 6, and 10 cm. The values of θ at the three depths were calculated as the product of gravimetric water contents and ρ_b measurements. Three replicated measurements were obtained at an average interval of 1.9 days (i.e., concurrently with ρ_b measurement).

d. Measuring λ with heat-pulse probes

To evaluate the λ estimates from the L14 model, HPPs were installed at 2-, 6-, and 10-cm depths to measure hourly λ with dual-probe heat-pulse theory (Bristow 2002). The HPP, built following the design of Ren et al. (2003), had three stainless-steel needles (4 cm long, 1.3 mm in diameter, and 6 mm spacing between adjacent needles) that were held in place with epoxy resin at one end. Each needle contained a thermocouple (type E, 50 μm in diameter) at the midpoint, and the central needle also contained a resistance wire heater. The HPP was inserted into undisturbed soil, with the central needle placed at the desired depth and the outer needles aligned vertically.

For each measurement, an 8-s heat pulse was generated with a 12-V battery to the resistance heater (heating power was in the range of 60–70 W m^{-1}), and the temperature changes were recorded simultaneously at a 1-s interval for 180 s. A datalogger (CR23X, Campbell Scientific, Logan, Utah) controlled the heating and data collection process. The λ values were estimated from the temperature change–time curve using a nonlinear regression technique (Welch et al. 1996). The ambient temperature drift was corrected by subtracting the background temperature from the temperature measurements (Jury and Bellantuoni 1976). The trend in

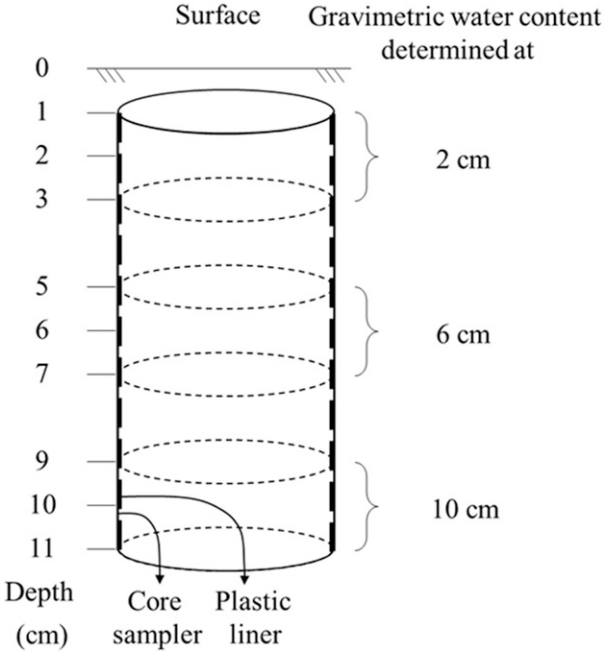

FIG. 1. Sketch of the soil core sample device for collecting and splitting soil samples into layers of 1–3, 5–7, and 9–11 cm, which were used to determine gravimetric water contents at the 2-, 6-, and 10-cm depths. The view is drawn approximately to scale.

background temperature was monitored with the outer needle for 60 s before initiating the heat pulse. Bristow et al. (1993) proposed another method for correction of ambient temperature drift by capturing the actual variation in background temperature. This method is recommended for use at very shallow soil depths where temperature can change dramatically and nonlinearly. The late-time fitting scheme of Lu et al. (2013) was used to minimize the influences of finite probe radius, finite probe heat capacity, and soil-probe thermal contact resistance.

e. Estimating soil heat flux using the gradient method

Soil heat fluxes at 2-, 6-, and 10-cm depths were determined using the gradient method (Sauer 2002). The λ value at each depth was either measured with an HPP λ_{HP} or estimated with the thermal conductivity model λ_m. For the modeling approach, the λ value at the 2-cm depth was estimated from ρ_b measurements of the 0–5-cm layer and TDR θ data at that depth. The λ values at the 6- and 10-cm depths were estimated from ρ_b data of the 5–10-cm layer and TDR θ measurements at each depth.

For the temperature measurements associated with the modeling approach, fine-wire thermocouples (type E, 50 μm in diameter) embedded in stainless-steel needles (4 cm long and 1.3 mm in diameter) were installed at 1-, 3-, 4-, 8-, and 12-cm depths to determine the temperature gradients ($\Delta T_m/\Delta z_m$) at 2-, 6-, and 10-cm depths, respectively. For the HPP method, the temperature gradients at depths of 2, 6, and 10 cm were calculated by dividing the temperature difference between the outer needles of an HPP by the needle spacing ($\Delta T_{HP}/\Delta z_{HP}$; Ochsner et al. 2006). Before installation, each HPP was calibrated in agar-stabilized water (5 g L^{-1}) in order to determine the apparent needle-to-needle spacing (Campbell et al. 1991).

Finally, heat flux data from a heat-pulse probe G_{HP} and G_m were determined as the product of λ_{HP} and $\Delta T_{HP}/\Delta z_{HP}$ and λ_m and $\Delta T_m/\Delta z_m$, respectively.

f. Error analysis

To evaluate the performance of the thermal conductivity model, we calculated the root-mean-square error (RMSE) and mean relative error (MRE) of λ_m against λ_{HP}:

$$\mathrm{RMSE} = \sqrt{\frac{1}{n}\sum(\lambda_{HP} - \lambda_m)^2} \quad \text{and} \tag{5}$$

$$\mathrm{MRE} = \frac{1}{n}\sum\left|(\lambda_{HP} - \lambda_m)/\lambda_{HP}\right|, \tag{6}$$

where n is the number of data points.

Similarly, to evaluate the λ model–based approach for estimating G_m, RMSE and MRE of G_m against G_{HP} were calculated as

$$\mathrm{RMSE} = \sqrt{\frac{1}{n}\sum(G_{HP} - G_m)^2} \quad \text{and} \tag{7}$$

$$\mathrm{MRE} = \frac{1}{n}\sum\left|(G_{HP} - G_m)/G_{HP}\right|. \tag{8}$$

3. Results and discussion

a. Field performance of the L14 thermal conductivity model

Figure 2 shows the time series of λ_m and λ_{HP} in the study period. The λ_m data were obtained based on hourly TDR θ data and assuming a constant bulk density ρ_{b-i}, corresponding to ρ_b measured at the beginning of the experiment. Both λ_m and λ_{HP} increased rapidly with increasing θ (after rainfall) and decreased gradually with soil drying. At 2 cm, λ values were relatively small but varied considerably with time. At the 6- and 10-cm depths, λ had larger magnitude and slighter temporal variations as compared to that of the 2-cm depth. This was caused by the fact that during the wetting–drying cycles, θ at 2 cm was generally smaller (0.09 cm^3 cm^{-3} on average) but varied from 0.03 to 0.22 cm^3 cm^{-3}, while it was larger and more stable at 6- and 10-cm depths. These observations were consistent with previous reports that near-surface λ correlated positively with θ (Peng et al. 2015).

The RMSE and MRE of λ_m results (against λ_{HP}) were 0.05 W m^{-1} K^{-1} and 3.3% at the 6-cm depth and 0.05 W m^{-1} K^{-1} and 3.7% at the 10-cm depth (Table 2). Linear regression analysis between λ_m and λ_{HP} produced lines with close-to-unity slopes (0.94–0.95) and high goodness of fit (coefficient of determination r^2 range of 0.91–0.92). Thus, the L14 model produced reliable λ estimates at the deeper layers. At the 2-cm depth, however, larger λ_m errors were observed: the RMSE and MRE were 0.08 W m^{-1} K^{-1} and 7.4%, respectively (Table 2). The discrepancies between λ_m and λ_{HP} became greater after DOY 265–266, during which a 19-mm rainfall occurred (Fig. 2a). These discrepancies are discussed further in following sections.

b. Soil heat flux estimates with modeled thermal conductivity

Comparisons of G_m and G_{HP} at 2-, 6-, and 10-cm depths are presented in Fig. 3 and Table 3. Generally, G_m and G_{HP} followed the same trend and responded similarly to temporal solar radiation and rainfall. The magnitude of soil heat flux decreased with increasing

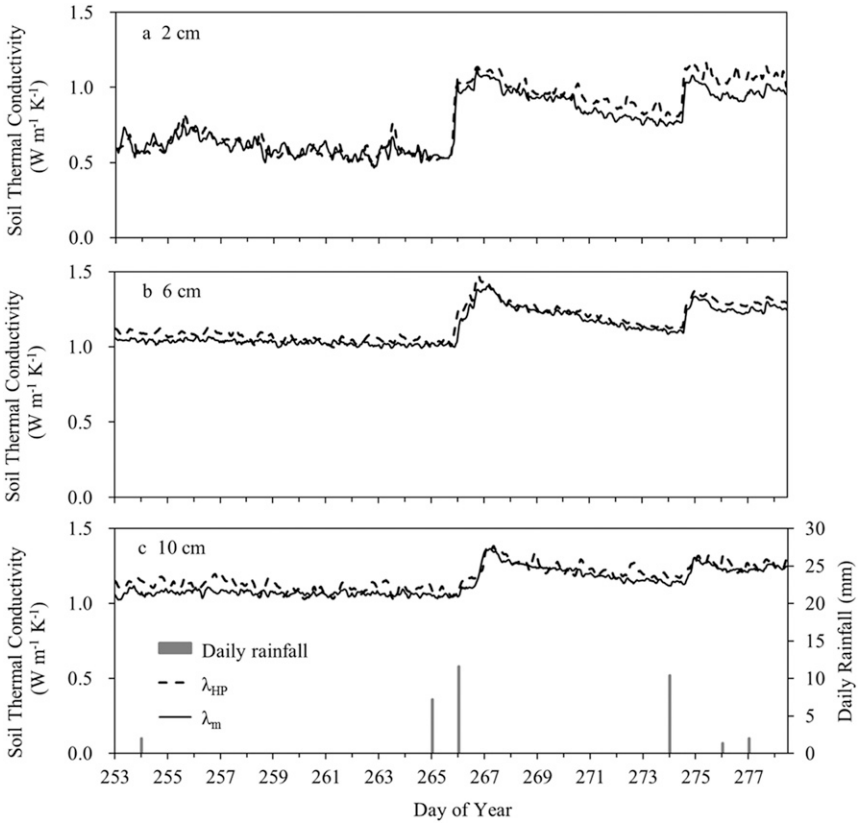

FIG. 2. Time series of soil thermal conductivity measured with heat-pulse probes and those estimated with the L14 model at (a) 2, (b) 6, and (c) 10 cm. Daily rainfall is also shown in (c).

depth: G_m and G_{HP} ranged from -80 to 220 W m^{-2} at 2 cm, from -60 to 160 W m^{-2} at 6 cm, and from -50 to 80 W m^{-2} at 10 cm, which was caused mainly by the attenuated soil temperature gradient with depth.

Compared to G_{HP} results, the errors of G_m estimates ranged from 4.7 W m^{-2} (12.0%) at 10-cm depth to 7.6 W m^{-2} (15.1%) at 2-cm depth. Linear regression between G_m and G_{HP} produced slopes close to unity (0.91–0.93) and high r^2 values (>0.98; Table 3). The good agreement between G_m and G_{HP} data indicates that measured T and model-estimated λ can be used in the gradient method to produce reliable G dynamics.

The discrepancies between G_m and G_{HP} were caused by the uncertainties in both $\Delta T_m/\Delta z_m$ and λ_m. The differences between $\Delta T_m/\Delta z_m$ and $T_{HP}/\Delta z_{HP}$ were 12%, 13%, and 12% at 2, 6, and 10 cm, respectively, which were caused mainly by the spatial variability of field soil temperature (the thermocouples array located about 15 cm from the HPP sensors) and the differences of sensor placement depth between thermocouples and HPP needles. The abovementioned methods for determining $\Delta T/\Delta z$, which assume that the near-surface T profiles are linear, have been used widely in practice (Kimball et al. 1976; Cobos and Baker 2003; Ochsner et al. 2006). Under field conditions, however, near-surface T is often distributed nonlinearly, and assuming a linear T gradient may lead to errors in G results. An alternative way is to obtain $\Delta T/\Delta z$ by fitting the temperature profile with exponential or high-order polynomial functions, and then determining $\Delta T/\Delta z$ from the derivatives. Further study is required to evaluate the performance of this alternative method and to identify the magnitude of G errors associated with neglecting nonlinearity of the T profiles near the surface.

The empirical nature of the L14 model may also bring in errors in λ_m estimates. The range of λ_m errors in this study were similar at 6- and 10-cm depths and were close

TABLE 2. RMSE, MRE, and linear regression statistics of soil thermal conductivity values estimated with the L14 model against those measured with heat-pulse probes at 2-, 6-, and 10-cm depths.

Depth (cm)	RMSE (W m^{-1} K^{-1})	MRE (%)	Slope	r^2
2	0.08	7.4	0.80	0.91
6	0.05	3.3	0.95	0.92
10	0.05	3.7	0.94	0.91

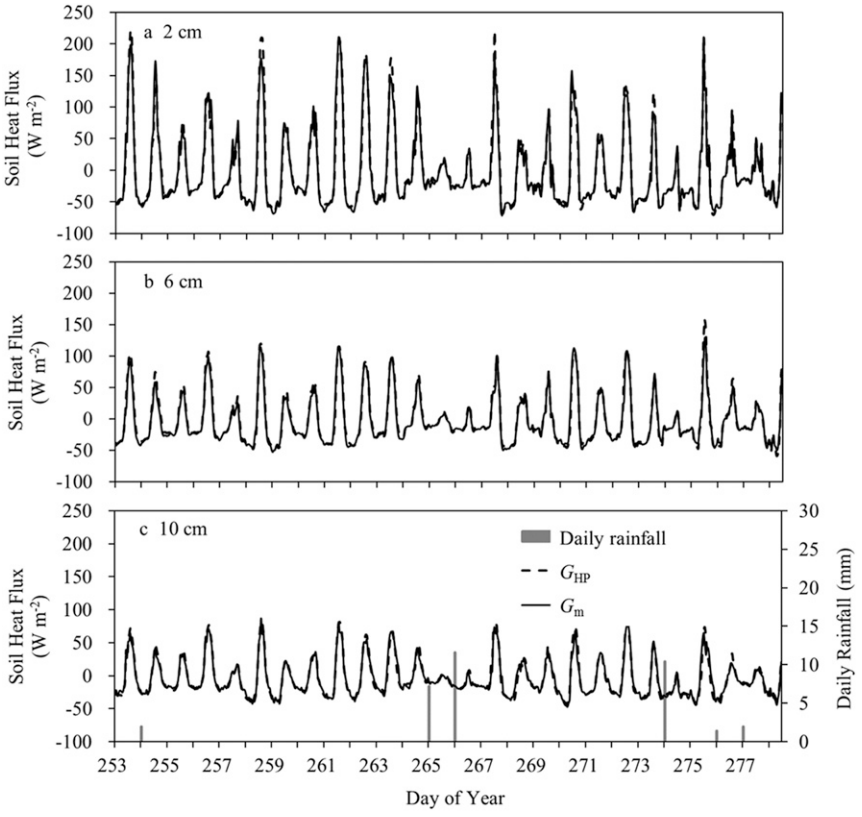

FIG. 3. Time series of soil heat flux measured with heat-pulse probe and thermal conductivity model–based values at (a) 2, (b) 6, and (c) 10 cm. Daily rainfall is also shown in (c).

to that obtained by L14 in laboratory tests against HPP data. At the 2-cm depth, however, the model provided an anomaly where the λ_m errors were nearly doubled compared to the deeper depths (Table 2), which resulted in the greatest discrepancies between G_m and G_{HP} (Table 3).

c. *Effects of variable soil bulk density on thermal conductivity and heat flux estimates*

In agricultural soils, ρ_b of the tilled layer varies with time after tillage or traffic (Alletto and Yves 2009; Liu et al. 2014), which may affect the transfers of gas, water, and energy at the soil–air interface. A few researchers have suggested the importance of accounting for temporal ρ_b (or soil porosity) changes in facilitating quantitative studies on soil gas (Han et al. 2014) or water movement (Moret and Arrúe 2007; Schwen et al. 2011). However, temporal changes of ρ_b are rarely considered when modeling λ and estimating G with the gradient method. Since λ depends largely on ρ_b (Farouki 1986; Bristow 2002), it is reasonable to assume that ignoring temporal dynamics of ρ_b could bias λ and the corresponding G estimates. In this section, we examined the temporal variability of ρ_b in the 0–5- and 5–10-cm layers and the subsequent effects on λ and G results.

During the study period, ρ_b increased from 1.27 to 1.39 g cm^{-3} in the 0–5-cm soil layer (Fig. 4a). The ρ_b increase appeared mainly after DOY 266, when there were two rainfall events during DOY 265–266 (19 mm) and on DOY 274 (10 mm). The soil bulk density of the 0–5-cm layer was around 1.27–1.29 g cm^{-3} before DOY 266, but increased almost linearly thereafter due to soil reconsolidation in the wetting–drying processes (Alletto and Yves 2009).

Figure 4b compares λ_{HP} with λ_m data estimated using initial bulk density (i.e., ρ_{b-i}; measured on DOY 253) and those using variable bulk densities ρ_{b-v} (Fig. 4a). When ρ_{b-i} was used in the model, a large discrepancy

TABLE 3. RMSE, MRE, and linear regression statistics of thermal conductivity model–based soil heat flux against those determined with heat-pulse probes at 2-, 6-, and 10-cm depths. Soil temperature gradients measured with thermocouples and heat-pulse probes were used for estimating Gm and GHP, respectively.

Depth (cm)	RMSE (W m^{-2})	MRE (%)	Slope	r^2
2	7.6	15.1	0.91	0.99
6	5.4	12.6	0.93	0.99
10	4.7	12.0	0.92	0.98

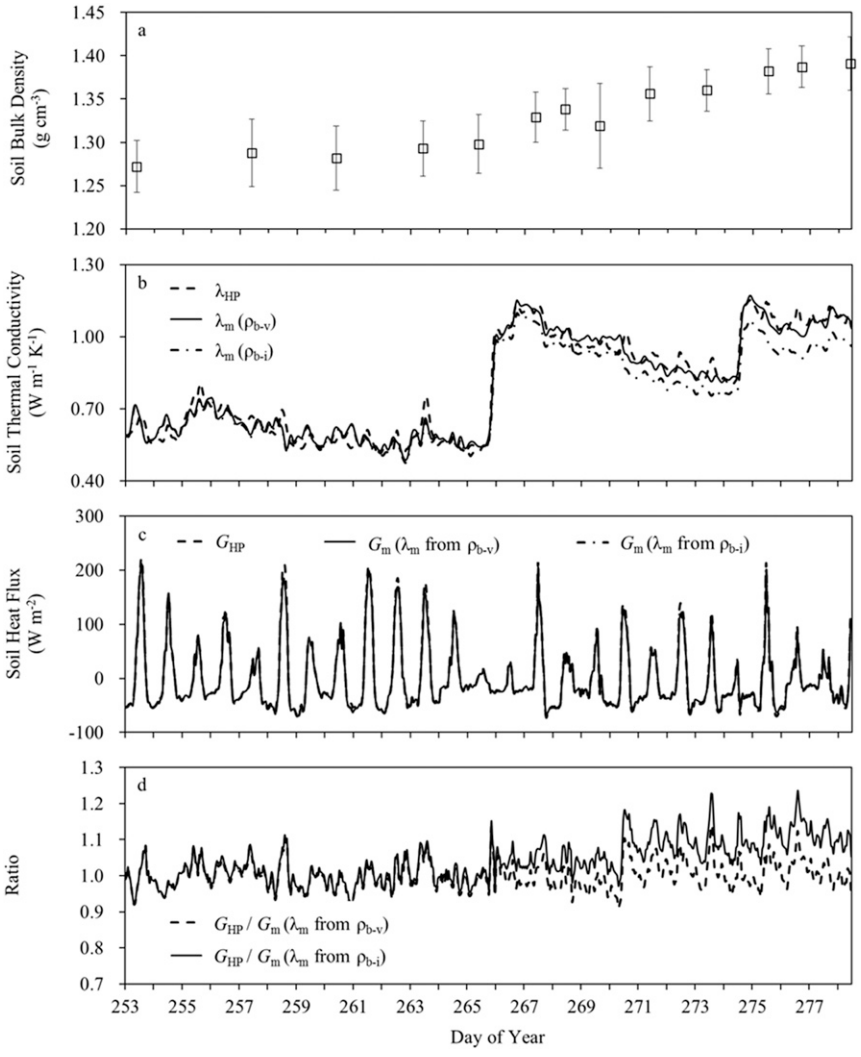

FIG. 4. Dynamics of (a) soil bulk density of the 0–5-cm soil layer, (b) soil thermal conductivity values measured with heat-pulse probes and those estimated with the L14 model, (c) soil heat flux at 2 cm determined with λ_{HP} (G_{HP}) and those with λ_m (G_m) using variable bulk density (ρ_{b-v}) and initial bulk density (ρ_{b-i}), and (d) the ratio of G_{HP} to G_m for λ_m (ρ_{b-v}) vs that of G_{HP} to G_m for λ_m (ρ_{b-i}) at 2 cm.

($0.08\,W\,m^{-1}\,K^{-1}$) was observed between λ_{HP} and λ_m values. When ρ_{b-v} was used, the accuracy of λ_m was increased (with errors decreased by $0.03\,W\,m^{-1}\,K^{-1}$ or almost 40%). The improvement in model performance was more apparent at the later part of the observation period (after DOY 266; Fig. 4b) when the differences between ρ_{b-v} and ρ_{b-i} became greater following the wetting–drying cycles discussed above.

It was not surprising that the accuracy of G_m estimates at the 2-cm depth was improved after accounting for the temporal variations of ρ_b in λ_m modeling (Fig. 4c). The errors in 2-cm depth G_m, after incorporating ρ_{b-v}, decreased to $5.9\,W\,m^{-2}$ (12.5%), which was smaller than errors with G_m based on ρ_{b-i} at the same depth, and similar to G_m errors observed at the 6- and 10-cm depths (12.0%–12.6%, Table 3).

The improvement in G_m estimates at the 2-cm depth was further illustrated with the ratio of G_{HP}/G_m (Fig. 4d). In the early study period (before DOY 264) when ρ_{b-v} was close to ρ_{b-i}, the G_m (ρ_{b-i}) and G_m (ρ_{b-v}) data agreed well with the G_{HP} values, and the two G_{HP}/G_m lines generally overlapped and fluctuated around 1. After DOY 266 when ρ_b increased gradually, the ρ_{b-i}-based G_{HP}/G_m line increased gradually and deviated substantially from 1, while the ρ_{b-v}-based G_{HP}/G_m line remained in the 0.9–1.1 range. Thus, using variable bulk density in the λ model produced more accurate G results in the near-surface layer.

An increase in ρ_b was also observed in the 5–10-cm layer, but to a much lesser extent: from 1.35 to 1.40 g cm^{-3} during the study period. At the 6-cm depth, using variable $\rho_{b\text{–}v}$ instead of $\rho_{b\text{–}i}$ led to a slight improvement in λ model performance (with a 0.01 W m^{-1} K^{-1} reduction in RMSE). RMSE of G_m estimates against G_{HP} measurements were decreased by 0.3 W m^{-2} after using λ_m estimates based on variable $\rho_{b\text{–}v}$. At 10-cm depth, using variable $\rho_{b\text{–}v}$ instead of $\rho_{b\text{–}i}$ led to a negligible change in λ model performance (<0.01 W m^{-1} K^{-1}), and thus also in G_m estimates (about 0.1 W m^{-2}).

d. *Cautions on application of the thermal conductivity model–based gradient method*

Accurate soil water content, texture, and bulk density are required for obtaining high-accuracy near-surface G data using the λ model–based gradient method. First, it is critical to monitor the temporal changes in θ. In this study, gravimetric sampling results θ_g at a 1.9-day sampling interval produced comparable λ_m data at the sampling times to that obtained with the TDR water contents θ_T (data not shown). Close examination of the data around rainfall events, however, showed that the sampling method failed to capture the dynamics of λ and G shortly after rainfall. For instance, a total of 19 mm rainfall occurred during the DOY 265–268 period, which led to a θ increase of 0.16 cm^3 cm^{-3} at 2-cm soil depth. In response, the λ at 2-cm depth increased rapidly and remained at about 1.0 W m^{-1} K^{-1} thereafter. For the periods when water content was not determined gravimetrically (e.g., the 2-day interval between the two discrete θ_g measurements in Fig. 5a), θ_g data were linearly interpolated with time to produce 1-h θ_g data and then 1-h λ_m estimates with the L14 model. When hourly λ_m (θ_g) estimates were used in the gradient method, the magnitude of G was underestimated by about 6 W m^{-2} (22%; dashed–dotted line in Fig. 5b) compared to the G_{HP} estimates (dashed line in Fig. 5b). This was especially clear around midnight of DOY 266 when λ increased significantly (up to 1.14 W m^{-1} K^{-1}, Fig. 5a) with rapid increase of θ. This error might exceed 50 W m^{-2} at midday in summer when soil temperature gradients are large in magnitude (e.g., about −180 K m^{-1} in maximum on days like DOY 257). On the other hand, by using the hourly θ_T data, the L14 model captured the rapid increase of λ and thus produced reliable G_m estimates (solid line in Fig. 5b), as indicated by the close agreement between G_m and G_{HP}. Similarly, Ochsner et al. (2007) indicated that gravimetric water content data could produce reliable soil volumetric heat capacity using the de Vries (1963) model, but they had inherent limitations in capturing the temporal changes of heat capacity.

Second, the L14 model [Eq. (4)] requires the quartz fraction, which is usually unavailable in meteorological and soil studies. Instead, many researchers use f_s for f_q (e.g., Peters-Lidard et al. 1998; Verhoef et al. 2012) with the assumption that sand is representative of quartz. In reality, quartz has a much larger thermal conductivity than many other soil minerals (8.4 vs 2.9 W m^{-1} K^{-1}; Farouki 1986), and f_q may differ considerably from f_s because quartz can exist at all particle sizes (Balland and Arp 2005). Thus, using f_s for f_q in the λ model may result in erroneous λ estimates (Bristow 1998).

To minimize errors associated with using f_s instead of f_q, L14 proposed a single-point correction for estimating the "correct" shape factor β. Rearranging Eq. (1), we have

$$\beta = \ln(\lambda_i - \lambda_{dry}) + \theta_i^{-\alpha}. \quad (9)$$

To use this correction method, a measured data point (θ_i, λ_i) along with ρ_b and soil clay fraction (for estimating α) are required. In this study, we determined the "correct" β using a λ measurement at an intermediate θ (0.09, 0.16, and 0.17 m^3 m^{-3} at 2-, 6-, and 10-cm depths, respectively), where the largest λ changes in response to β occurred (L14). Use of the corrected β slightly improved the accuracy of modeled λ (by 0.01 W m^{-1} K^{-1} on average) and that of the corresponding G_m estimates (by about 1 W m^{-2} on average). For the particular soil in this study, sand fraction was an acceptable proxy for quartz content. In practice, the single-point correction [Eq. (9)] is recommended for improving the performance of the L14 model when f_q is not available.

Finally, our field test suggested that in the 0–5-cm soil layer, a 0.12 g cm^{-3} ρ_b increase in the 25-day period led to an increase in G errors of about 2 W m^{-2}. In agricultural soils, significant temporal ρ_b change may occur in the surface soil layers. For example, Liu et al. (2014) reported that ρ_b increased from about 1.0 to 1.3 g cm^{-3} within 40 days after tillage. In such cases, temporal ρ_b changes should be accounted for in the λ model, or the errors in λ and G estimates could multiply. In this study, measuring ρ_b three times per week using the core method was frequent enough to capture the temporal variation of near-surface ρ_b. Recently, the thermo–time domain reflectometry sensor has been developed for monitoring in situ ρ_b dynamics. This technique allows for determination of ρ_b from concurrent measurement of soil thermal properties and θ (Ochsner et al. 2001; Liu et al. 2008, 2014). Additionally, for situations where dramatic temporal ρ_b variations occur, large changes in sensor depth may occur in circumstances with significant temporal ρ_b variations. This could cause large uncertainties in estimates of soil-surface heat flux. Keeping

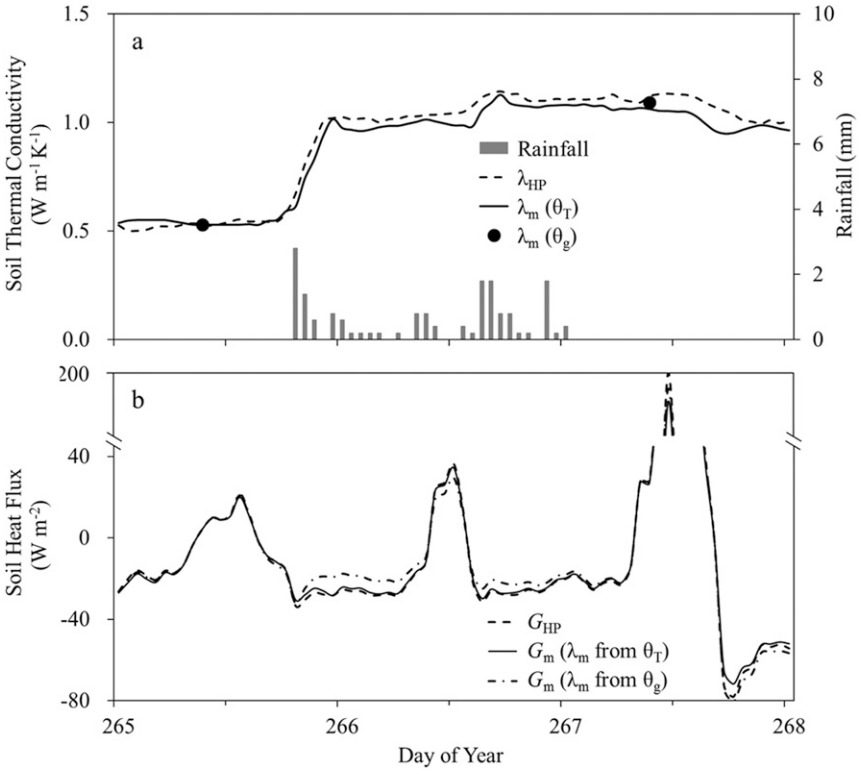

FIG. 5. At 2-cm depth during DOY 265 and 268 (a) time series of soil thermal conductivity measured with the heat-pulse probes and those estimated with the L14 model using hourly TDR data and gravimetric values and (b) the time series of the corresponding soil heat flux determined with λ_{HP} (G_{HP}) and those determined with λ_m (G_m) during the DOY 265 and 268 period. Hourly rainfall is also shown in (a).

the sensors stable using supporting structures and monitoring the change in surface elevation could provide useful information about sensor depth changes with time. This information can be used in soil heat flux and heat storage calculations, and thus, may reduce errors in soil-surface heat flux determination.

4. Summary and conclusions

In this study, we evaluated the potential of using modeled λ with the gradient method for determining G at shallow soil depths. The L14 model was used to estimate λ from soil texture, θ, and ρ_b. Comparisons between G measurements from the HPP and those based on the λ model revealed that the gradient method with modeled λ could produce reliable near-surface G. Use of the λ model instead of an HPP had the advantages of fewer requirements for instruments, data collection, and postprocessing.

Compared to the 6- and 10-cm depths, relatively larger G errors were observed at the 2-cm depth, which was mainly due to λ modeling errors by ignoring temporal ρ_b changes. The accuracies of λ and the corresponding G estimates were improved after accounting for the temporal changes in ρ_b. In addition, continuous θ measurements obtained using in situ techniques (e.g., TDR) are required to capture the temporal variations of λ and G, especially during wetting–drying processes when near-surface water content can change rapidly. A single-point correction can be used to mitigate λ modeling errors caused by inaccurate soil mineralogy information. Further field evaluations for a range of soils and surface conditions are required to identify the accuracy and reliability of the use of the gradient method with model-estimated λ.

Acknowledgments. This research was supported by the National Natural Science Foundation of China (41271238, Tusheng Ren), the National Key Technology Research and Development Program of China (2015CB150403, Tusheng Ren), U.S. National Science Foundation (Grant 1623806, Robert Horton and Joshua Heitman), Army Research Office (Award W911NF1610287, Joshua Heitman and Robert Horton),

and USDA-NIFA (Multi-State Project 3188, Robert Horton and Joshua Heitman).

REFERENCES

Abu-Hamdeh, N. H., and R. C. Reeder, 2000: Soil thermal conductivity: Effects of density, moisture, salt concentration, and organic matter. *Soil. Sci. Soc. Amer. J.*, **64**, 1285–1290, doi:10.2136/sssaj2000.6441285x.

Alletto, L., and C. Yves, 2009: Temporal and spatial variability of soil bulk density and near-saturated hydraulic conductivity under two contrasted tillage management systems. *Geoderma*, **152**, 85–94, doi:10.1016/j.geoderma.2009.05.023.

Balland, V., and P. Arp, 2005: Modelling soil thermal conductivities over a wide range of conditions. *J. Environ. Eng. Sci.*, **4**, 549–558, doi:10.1139/s05-007.

Bristow, K. L., 1998: Measurement of thermal properties and water content of unsaturated sandy soil using dual-probe heat-pulse probes. *Agric. For. Meteor.*, **89**, 75–84, doi:10.1016/S0168-1923(97)00065-8.

——, 2002: Thermal conductivity. *Methods of Soil Analysis: Part 4, Physical Methods*, J. H. Dane and G. C. Topp, Eds., SSSA Book Series, Vol. 5, Soil Science Society of America, 1209–1226.

——, G. S. Campbell, and C. Calissendorff, 1993: Test of a heat-pulse probe for measuring changes in soil water content. *Soil. Sci. Soc. Amer. J.*, **57**, 930–934, doi:10.2136/sssaj1993.03615995005700040008x.

Campbell, G. S., C. Calissendorff, and J. H. Williams, 1991: Probe for measuring soil specific heat using a heat-pulse method. *Soil. Sci. Soc. Amer. J.*, **55**, 291–293, doi:10.2136/sssaj1991.03615995005500010052x.

Chung, S. O., and R. Horton, 1987: Soil heat and water flow with a partial surface mulch. *Water Resour. Res.*, **23**, 2175–2186, doi:10.1029/WR023i012p02175.

Cobos, D. R., and J. M. Baker, 2003: In situ measurement of soil heat flux with the gradient method. *Vadose Zone J.*, **2**, 589–594, doi:10.2136/vzj2003.5890.

Côté, J., and J. M. Konrad, 2005: A generalized thermal conductivity model for soils and construction materials. *Can. Geotech. J.*, **42**, 443–458, doi:10.1139/t04-106.

de Vries, D. A., 1963: Thermal properties of soils. *Physics of Plant Environment*, W. R. van Wijk, Ed., North-Holland Publishing, 210–235.

Dong, J., S. C. Steele-Dunne, J. Judge, and N. van de Giesen, 2015: A particle batch smoother for soil moisture estimation using soil temperature observations. *Adv. Water Resour.*, **83**, 111–122, doi:10.1016/j.advwatres.2015.05.017.

Evett, S. R., N. Agam, W. P. Kustas, P. D. Colaizzi, and R. C. Schwartz, 2012: Soil profile method for soil thermal diffusivity, conductivity and heat flux: Comparison to soil heat flux plates. *Adv. Water Resour.*, **50**, 41–54, doi:10.1016/j.advwatres.2012.04.012.

Farhadi, L., D. Entekhabi, G. Salvucci, and J. Sun, 2014: Estimation of land surface water and energy balance parameters using conditional sampling of surface states. *Water Resour. Res.*, **50**, 1805–1822, doi:10.1002/2013WR014049.

Farouki, O. T., 1986: *Thermal Properties of Soils: Series on Rock and Soil Mechanics*. Trans Tech Publications, 136 pp.

Ferré, T. P. A., and G. C. Topp, 2002: Time domain reflectometry. *Methods of Soil Analysis: Part 4, Physical Methods*, J. H. Dane and G. C. Topp, Eds., SSSA Book Series, Vol. 5, Soil Science Society of America, 434–446.

Gee, G. W., and D. Or, 2002: Particle-size analysis. *Methods of Soil Analysis: Part 4, Physical Methods*, J. H. Dane and G. C. Topp, Eds., SSSA Book Series, Vol. 5, Soil Science Society of America, 255–293.

Gentine, P., D. Entekhabi, and B. Heusinkveld, 2012: Systematic errors in ground heat flux estimation and their correction. *Water Resour. Res.*, **48**, W09541, doi:10.1029/2010WR010203.

Grossman, R. B., and T. G. Reinsch, 2002: Bulk density and linear extensibility. *Methods of Soil Analysis: Part 4, Physical Methods*, J. H. Dane and G. C. Topp, Eds., SSSA Book Series, Vol. 5, Soil Science Society of America, 201–228.

Han, W., Y. Gong, T. Ren, and R. Horton, 2014: Accounting for time-variable soil porosity improves the accuracy of the gradient method for estimating soil carbon dioxide production. *Soil. Sci. Soc. Amer. J.*, **78**, 1426–1433, doi:10.2136/sssaj2013.12.0542.

Heitman, J. L., R. Horton, T. J. Sauer, and T. M. DeSutter, 2008: Sensible heat observations reveal soil-water evaporation dynamics. *J. Hydrometeor.*, **9**, 165–171, doi:10.1175/2007JHM963.1.

——, ——, ——, T. Ren, and X. Xiao, 2010: Latent heat in soil heat flux measurements. *Agric. For. Meteor.*, **150**, 1147–1153, doi:10.1016/j.agrformet.2010.04.017.

Johansen, O., 1975: Thermal conductivity of soils. Ph.D. thesis, University of Trondheim, 236 pp.

Jury, W. A., and B. Bellantuoni, 1976: A background temperature correction for thermal conductivity probes. *Soil. Sci. Soc. Amer. J.*, **40**, 608–610, doi:10.2136/sssaj1976.03615995004000040040x.

Kimball, B. A., R. D. Jackson, F. S. Nakayama, S. B. Idso, and R. J. Reginato, 1976: Soil-heat flux determination: Temperature gradient method with computed thermal conductivities. *Soil. Sci. Soc. Amer. J.*, **40**, 25–28, doi:10.2136/sssaj1976.03615995004000010011x.

Liu, G., L. Zhao, M. Wen, X. Chang, and K. Hu, 2013: An adiabatic boundary condition solution for improved accuracy of heat-pulse measurement analysis near the soil–atmosphere interface. *Soil. Sci. Soc. Amer. J.*, **77**, 422–426, doi:10.2136/sssaj2012.0187n.

Liu, X., T. Ren, and R. Horton, 2008: Determination of soil bulk density with thermo–time domain reflectometry sensors. *Soil. Sci. Soc. Amer. J.*, **72**, 1000–1005, doi:10.2136/sssaj2007.0332.

——, S. Lu, R. Horton, and T. Ren, 2014: In situ monitoring of soil bulk density with a thermo-TDR sensor. *Soil. Sci. Soc. Amer. J.*, **78**, 400–407, doi:10.2136/sssaj2013.07.0278.

Lu, S., T. Ren, Y. Gong, and R. Horton, 2007: An improved model for predicting soil thermal conductivity from water content at room temperature. *Soil. Sci. Soc. Amer. J.*, **71**, 8–14, doi:10.2136/sssaj2006.0041.

Lu, Y. L., Y. J. Wang, and T. Ren, 2013: Using late time data improves the heat–pulse method for estimating soil thermal properties with the pulsed infinite line source theory. *Vadose Zone J.*, **12**, doi:10.2136/vzj2013.01.0011.

——, S. Lu, R. Horton, and T. Ren, 2014: An empirical model for estimating soil thermal conductivity from texture, water content, and bulk density. *Soil. Sci. Soc. Amer. J.*, **78**, 1859–1868, doi:10.2136/sssaj2014.05.0218.

Mayocchi, C. L., and K. L. Bristow, 1995: Soil surface heat flux: Some general questions and comments on measurements. *Agric. For. Meteor.*, **75**, 43–50, doi:10.1016/0168-1923(94)02198-S.

McInnes, K. J., 2002: Soil heat: Temperature. *Methods of Soil Analysis: Part 4, Physical Methods*, J. H. Dane and G. C. Topp,

Eds., SSSA Book Series, Vol. 5, Soil Science Society of America, 1183–1199.

Moret, D., and J. L. Arrúe, 2007: Dynamics of soil hydraulic properties during fallow as affected by tillage. *Soil Tillage Res.*, **96**, 103–113, doi:10.1016/j.still.2007.04.003.

Ochsner, T. E., R. Horton, and T. Ren, 2001: A new perspective on soil thermal properties. *Soil. Sci. Soc. Amer. J.*, **65**, 1641–1647, doi:10.2136/sssaj2001.1641.

——, T. J. Sauer, and R. Horton, 2006: Field tests of the soil heat flux plate method and some alternatives. *Agron. J.*, **98**, 1005–1014, doi:10.2134/agronj2005.0249.

——, ——, and ——, 2007: Soil heat capacity and heat storage measurements in energy balance studies. *Agron. J.*, **99**, 311–319, doi:10.2134/agronj2005.0103S.

Peng, X., J. Heitman, R. Horton, and T. Ren, 2015: Field evaluation and improvement of the plate method for measuring soil heat flux density. *Agric. For. Meteor.*, **214–215**, 341–349, doi:10.1016/j.agrformet.2015.09.001.

Peters-Lidard, C. D., E. Blackburn, X. Liang, and E. F. Wood, 1998: The effect of soil thermal conductivity parameterization on surface energy fluxes and temperature. *J. Atmos. Sci.*, **55**, 1209–1224, doi:10.1175/1520-0469(1998)055<1209:TEOSTC>2.0.CO;2.

Ren, T., T. E. Ochsner, and R. Horton, 2003: Development of thermo–time domain reflectometry for vadose zone measurements. *Vadose Zone J.*, **2**, 544–551, doi:10.2136/vzj2003.5440.

Sauer, T. J., 2002: Heat flux density. *Methods of Soil Analysis: Part 4, Physical Methods*, J. H. Dane and G. C. Topp, Eds., SSSA Book Series, Vol. 5, Soil Science Society of America, 1233–1248.

——, and R. Horton, 2005: Soil heat flux. *Micrometeorology in Agricultural Systems*, *Agronomy Monogr.*, No. 47, American Society of Agronomy, 131–154.

Schwen, A., G. Bodner, P. Scholl, G. D. Buchan, and W. Loiskandl, 2011: Temporal dynamics of soil hydraulic properties and the water-conducting porosity under different tillage. *Soil Tillage Res.*, **113**, 89–98, doi:10.1016/j.still.2011.02.005.

Topp, G. C., J. L. Davis, and A. P. Annan, 1980: Electromagnetic determination of soil water content: Measurements in coaxial transmission lines. *Water Resour. Res.*, **16**, 574–582, doi:10.1029/WR016i003p00574.

Verhoef, A., C. Ottlé, B. Cappelaere, T. Murray, S. Saux-Picart, M. Zribi, and D. Ramier, 2012: Spatio-temporal surface soil heat flux estimates from satellite data; Results for the AMMA experiment at the Fakara (Niger) supersite. *Agric. For. Meteor.*, **154–155**, 55–66, doi:10.1016/j.agrformet.2011.08.003.

Wang, Z. H., and E. Bou-Zeid, 2012: A novel approach for the estimation of soil ground heat flux. *Agric. For. Meteor.*, **154–155**, 214–221, doi:10.1016/j.agrformet.2011.12.001.

Welch, S. M., G. J. Kluitenberg, and K. L. Bristow, 1996: Rapid numerical estimation of soil thermal properties for a broad class of heat-pulse emitter geometries. *Meas. Sci. Technol.*, **7**, 932–938, doi:10.1088/0957-0233/7/6/012.

Zhang, X., J. Heitman, R. Horton, and T. Ren, 2014: Measuring near-surface soil thermal properties with the heat-pulse method: Correction of ambient temperature and soil–air interface effects. *Soil. Sci. Soc. Amer. J.*, **78**, 1575–1583, doi:10.2136/sssaj2014.01.0014.